Dynamics of Continuous, Discrete and Impulsive Systems
Series **B:** *Applications & Algorithms* **22 (2015)** 359-379

A MATHEMATICAL MODEL FOR HIGH PATHOGENICITY AVIAN INFLUENZA VIRUSES EMERGING FROM OUTBREAKS WITH LOW PATHOGENICITY AVIAN INFLUENZA VIRUSES

Jianjun Paul Tian[1], Junping Shi[2], and Jingan Cui[3]

[1] Department of Mathematical Sciences
New Mexico State University, Las Cruces, New Mexico 88001, USA

[2] Department of Mathematics
College of William and Mary, Williamsburg, Virginia, 23187-8795, USA

[3] School of Science and Department of Mathematics
Beijing University of Civil Engineering and Architecture, Beijing 100044, P. R. China

Abstract. In this article, we establish a mathematical model for a complexity phenomenon that emerges from epidemiology. After the low pathogenicity avian influenza (LPAI) A virus (H5N2) outbreaks, most of time the high pathogenicity avian influenza (HPAI) viruses will emerges. This superinfection property is a typical complexity emerging from a system. Our model is based on traditional mathematical epidemiology models, experimental and field evidences. It has several submodels which are traditional SEIR models or SIR models. We analyze our model and their submodels. We carry out comparisons between model predictions and experimental data, and answer several important biological questions with our model. In addition, the complexity property is not derived from bifurcation theory.

Keywords. epidemiology, influenza, emergence, H5N2, pathogenicity

AMS (MOS) subject classification: 92B05, 34A99

1 Introduction

Complexity is a common phenomenon in ecological systems. Most of mathematical descriptions for complexity use bifurcation theory where systems are described by differential equations. In disease ecology, particulary, in epidemiology, although it seems common that a new strain of infectious virus emerges from the spreading of other viral infection in the same population, a mathematical description seems lack. In this study, we establish a mathematical model for emergence of high pathogenicity avian influenza virus from outbreaks of low pathogenicity avian influenza viruses. There is a parameter designed for emerging of the complexity. When this parameter is zero, the system is for the spreading of low pathogenicity avian

influenza viruses. When this parameter is positive, high pathogenicity avian influenza viruses emerge. The model is a system coupled with two systems. This emergence of the complexity is not derived from bifurcation theory.

Wild waterfowl are considered as natural hosts for all known subtypes of influenza A viruses and believed to have carried these viruses for centuries with none or limited harm [28, 32]. However, domestic poultry, such as turkeys and chickens, can become very sick and die from avian influenza, and some avian influenza A viruses also can cause serious disease and death in wild birds [1, 2].

Infected birds shed influenza virus in their saliva, nasal secretions, and feces. Susceptible birds become infected when they have contact with contaminated secretions or excretions or with surfaces that are contaminated with secretions or excretions from infected birds. Domesticated birds may become infected with avian influenza virus through direct contact with infected waterfowl or other infected poultry, or through contact with surfaces (such as dirt or cages) or materials (such as water or food) that have been contaminated with the virus [28].

Infection with avian influenza A viruses in domestic poultry causes two main forms of disease that are distinguished by low and high extremes of virulence [29]. Correspondingly, Avian influenza A virus strains are further classified as low pathogenic (LPAI) or highly pathogenic (HPAI) on the basis of specific molecular genetic and pathogenesis criteria. Most avian influenza A viruses are LPAI viruses, and are associated with low pathogenic form of disease that may go undetected and usually causes only mild symptoms (such as ruffled feathers and a drop in egg production). In contrast, HPAI viruses are associated with highly pathogenic form of disease that can cause severe illness and high mortality. This highly pathogenic form of infection spreads more rapidly through flocks of poultry. This form may cause disease that affects multiple internal organs and has a mortality rate that can reach 90-100% often within two days.

One intriguing characteristic is that high pathogenicity avian influenza (HPAI) viruses can emerge from outbreaks with low pathogenicity avian influenza (LPAI) viruses. One example is the outbreak of LPAI in chickens in Pennsylvania in 1983 [4]. This outbreak started in April 1983 with a low pathogenicity virus that caused only limited death. By October 1983 the virus circulating in the infected chicken population had transformed into a state of high pathogenicity, HPAI virus, which caused a 80% mortality. In 1994, an outbreak of LPAI in Mexico had a similar transformation occurrence [14]. The most recent outbreak of such a transformation occurrence is the outbreak of HPAI H7N1 in December 1999 in Italian that started as an outbreak of LPAI H7N1 in April of the same year [8]. During these outbreaks two processes can be distinguished, one is the HPAI virus arises during the LPAI outbreak and the other one is the HPAI supersedes the LPAI. Hence the following questions arise naturally:

1. How do the HPAI viruses arise from the outbreak of the LPAI viruses?

2. Are animals infected by HPAI virus more infectious than animals infected by LPAI virus?

3. Are animals previously infected with LPAI virus protected against infection with HPAI virus?

4. Is HPAI virus able to spread in a population in which LPAI is circulating or has circulated before?

5. How many animals should have had an infection with LPAI virus in order to prevent an outbreak of HPAI virus?

In [29] J. A. Van Der Goot, et al. asked similar questions. By means of transmission experiments, they compared the transmission characteristics in poultry of LPAI H5N2 (A/Chicken/Pennsylvania/83) and corresponding HPAI virus and attempted to answer those questions. In the present paper, we set up a mathematical model, compare it with the discrete experimental data in [29], and provide answers to those questions.

The mathematical modeling of transmission of avian influenza A viruses is an important current research topic. Related approaches can be found in [11, 12, 13, 19, 20, 6, 18, 27, 5]. One of the mathematical tools we use in our analysis is the Lyapunov function technique for SIR and SEIR type epidemic models, which has been further developed in recent years, for example, [15, 21, 22, 23, 24, 25].

The rest of the paper is organized as follows. In Section 2, the model is described. In Section 3, basic dynamic behaviors of the model are analyzed. In Section 4, we compare the model predictions with experimental data, and answer the questions. The paper is concluded in section 5.

2 Model description

We use a well-known compartmental model approach [3, 7, 16, 17]. The population of animals under consideration is divided into several disjoint classes. The susceptible class S consists of those individuals who can incur the disease but are not yet infected. When there is an adequate contact of a susceptible with the infective including direct contact and contact with surface or materials that have been contaminated with viruses shed from an infective, the susceptible enters the exposed class E of those in the latent period, who are infected but not yet infectious. After the latent period ends, the individual enters the class I of the infective, who are infectious in the sense that they are capable of transmitting the infection. When the infectious period ends, the individual enters the recovered class R consisting of those with permanent infection-acquired immunity. We work with classic SEIR model framework which is based on incidence principle [16]. Since there are two strains, LPAI and HPAI, each of them has its own compartment classes. More specifically, LPAI has latent class E_l, infectious class I_l and recovered

class R_l; HPAI has latent class E_h, infectious class I_h and recovered class R_h and an additional class X_h of dead individuals. It is reasonable to assume that an individual who is susceptible to LPAI is also susceptible to HPAI, and an individual who is susceptible to HPAI is also susceptible to LPAI. So there is one common susceptible class S. See the model diagram in Figure 1.

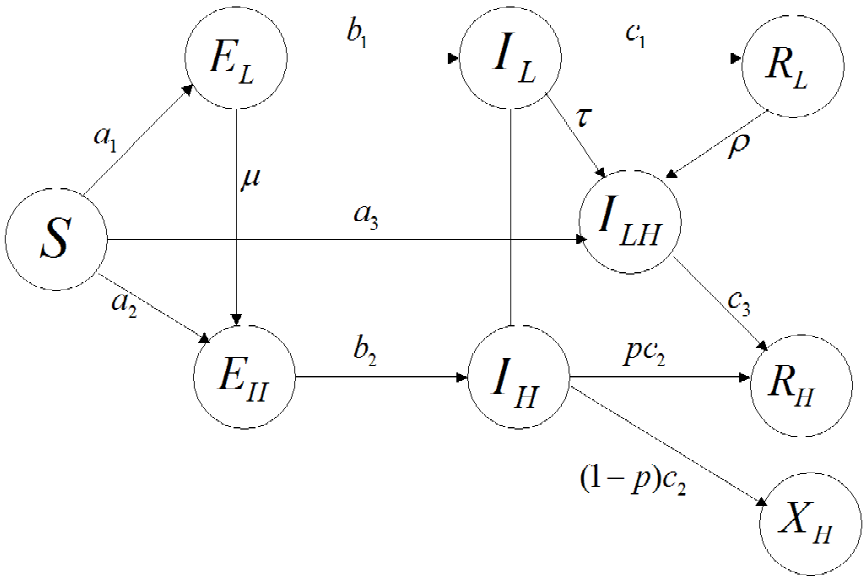

Figure 1: A compartmental diagram for emergence of high pathogenicity avian influenza virus from outbreaks with low pathogenicity avian influenza virus.

In order to consider the emergence of HPAI viruses from outbreaks with LPAI viruses, the following assumption are made:

1. An individual infected with LPAI virus can be infected by HPAI virus again, and become a superinfective, I_{lh}.
2. A superinfective can transmit infection to susceptible individuals.
3. A superinfective can enter the recovered class R_h.
4. A superinfective can transmit infection to individuals who is recovered from LPAI.
5. LPAI viruses can evolve or mutate into HPAI viruses during the latent period of LPAI viruses infection with animals.

The first four assumptions are based on experimental evidences. In [29], they performed three sets of experiments: experiments with LPAI H5N2

viruses, experiments with HPAI H5N2 viruses, and experiments with HPAI H5N2 viruses but contact animals were previously infected with LPAI H5N2 viruses. They found that none of infected contact animals die in the third set experiments, and they all become recovered. So we assume that all superinfective can enter the recovered class R_h.

All avian influenza A viruses are RNA viruses. Since RNA viruses do not have DNA polymerases which can find and fix mistakes, and therefore are unable to conduct DNA repair of damaged genetic material, then RNA viruses have very high mutation rates. In particular, influenza A viruses can mutate in two different ways: antigenic drift and antigenic shift. Antigenic drift refers to small, gradual changes that occur through point mutations in two genes that contain the genetic material to produce the main surface proteins, hemagglutinin, and neuraminidase. These point mutations occur unpredictably and result in minor changes to these surface proteins. Antigenic drift produces new virus strains that may not be recognized by antibodies to earlier influenza strains. Antigenic shift refers to an abrupt, major change to produce a novel influenza A virus subtype that was not currently circulating among the population. Influenza A viruses are mutating by antigenic drift all the time, but antigenic shift happens only occasionally. For simplicity, we assume that the mutation from LPAI viruses to HPAI viruses happens during the latent period of LPAI virus infection.

The model equations are given based on all assumptions above:

$$\frac{dS}{dt} = -a_1\frac{I_l}{N}S - a_2\frac{I_h}{N}S - a_3\frac{I_{lh}}{N}S, \tag{1}$$

$$\frac{dE_l}{dt} = a_1\frac{I_l}{N}S - b_1E_l - \mu E_l, \tag{2}$$

$$\frac{dE_h}{dt} = a_2\frac{I_h}{N}S - b_2E_l + \mu E_l, \tag{3}$$

$$\frac{dI_l}{dt} = b_1E_l - \tau\frac{I_lI_h}{N} - c_1I_l, \tag{4}$$

$$\frac{dI_h}{dt} = b_2E_h - c_2I_h, \tag{5}$$

$$\frac{dI_{lh}}{dt} = \tau\frac{I_lI_h}{N} + a_3\frac{I_{lh}}{N}S + \rho\frac{I_h}{N}R_l - c_3I_{lh}, \tag{6}$$

$$\frac{dR_l}{dt} = c_1I_l - \rho\frac{I_h}{N}R_l, \tag{7}$$

$$\frac{dR_h}{dt} = pc_2I_h + c_3I_{lh}, \tag{8}$$

$$\frac{dX_h}{dt} = (1-p)c_2I_h. \tag{9}$$

3 Model analysis

The model (1)-(9) describes three infections: infection with LPAI viruses, infection with HPAI viruses, and superinfection with LPAI viruses first and then with HPAI viruses. In this section, we analyze the dynamics of the model to understand how these infection emerge. Because the total population size $N = S(t) + E_l(t) + I_l(t) + R_l(t) + E_h(t) + I_h(t) + R_h(t) + I_{lh}(t) + X_h(t)$ remains a constant, we scale the variables:

$$\begin{aligned} s(t) &= \frac{S(t)}{N},\ i_{12}(t) = \frac{I_{lh}(t)}{N},\ x(t) = \frac{X_h(t)}{N}, \\ e_1(t) &= \frac{E_l(t)}{N},\ i_1(t) = \frac{I_l(t)}{N},\ r_1(t) = \frac{R_l(t)}{N}, \\ e_2(t) &= \frac{E_h(t)}{N},\ i_2(t) = \frac{I_h(t)}{N},\ r_2(t) = \frac{R_h(t)}{N}. \end{aligned} \tag{10}$$

And the new system is

$$\frac{ds}{dt} = -a_1 i_1 s - a_2 i_2 s - a_3 i_{12} s, \tag{11}$$

$$\frac{de_1}{dt} = a_1 i_1 s - b_1 e_1 - \mu e_1, \tag{12}$$

$$\frac{de_2}{dt} = a_2 i_2 s - b_2 e_2 + \mu e_1, \tag{13}$$

$$\frac{di_1}{dt} = b_1 e_1 - \tau i_1 i_2 - c_1 i_1, \tag{14}$$

$$\frac{di_2}{dt} = b_2 e_2 - c_2 i_2, \tag{15}$$

$$\frac{di_{12}}{dt} = \tau i_1 i_2 + a_3 i_{12} s + \rho i_2 r_1 - c_3 i_{12}, \tag{16}$$

$$\frac{dr_1}{dt} = c_1 i_1 - \rho i_2 r_1, \tag{17}$$

$$\frac{dr_2}{dt} = p c_2 i_2 + c_3 i_{12}, \tag{18}$$

$$\frac{dx}{dt} = (1-p) c_2 i_2. \tag{19}$$

3.1 Basic dynamics

The basic dynamics of the system is described as follows:

Theorem 3.1. *Consider the system* (11)-(19). *Suppose that the parameters satisfy* $b_i, c_i > 0$, $a_i, \rho, p, \mu \geq 0$. *Then*

1. *The positive hyperplane*

$$\begin{aligned} H = \{&(s, e_1, e_2, i_1, i_2, i_{12}, r_1, r_2, x) \in \mathbb{R}^9_+ : \\ &s + e_1 + e_2 + i_1 + i_2 + i_{12} + r_1 + r_2 + x = 1\} \end{aligned} \tag{20}$$

is invariant for the solutions of (11)-(19)*, where* $\mathbb{R}^9_+$ *is the non-negative octant so that each coordinate is nonnegative;*

2. *There is no interior equilibrium point of* (11)-(19) *in* $\mathbb{R}^9_+$*, and a point in* $\mathbb{R}^9_+$ *is an equilibrium point of* (11)-(19) *if and only if* $e_1 = e_2 = i_1 = i_2 = i_{12} = 0$ *and* $s + r_1 + r_2 + x = 1$.

3. *Suppose that* $s(0) > 0$, $i_1(0) + i_2(0) + i_{12}(0) > 0$ *and* $s(0) + e_1(0) + e_2(0) + i_1(0) + i_2(0) + i_{12}(0) + r_1(0) + r_2(0) + x(0) = 1$*, then there exist two equilibrium points* $\mathbf{P}^{\pm} = (s^{\pm}, 0, 0, 0, 0, 0, r_1^{\pm}, r_2^{\pm}, x^{\pm})$ *of* (11)-(19) *in* $\mathbb{R}^9_+$ *such that* $s^- > s^+$, $r_2^- < r_2^+$*, and* $x^- < x^+$*, and the corresponding non-negative solution* $\mathbf{P}(t)$ *satisfies*

$$\lim_{t\to-\infty} \mathbf{P}(t) = \mathbf{P}^-, \quad \lim_{t\to\infty} \mathbf{P}(t) = \mathbf{P}^+. \tag{21}$$

Proof. In the following, we denote a solution of (11)-(19) with non-negative initial value $\mathbf{P}_0 = (P_i(0))_{i=1}^9$ by $\mathbf{P}(t) = (P_i(t))_{i=1}^9$. From the previous remark, we know that the sum of all sub-populations is invariant. If a solution reaches the boundary of H, then at least one component $P_i(t)$ of $\mathbf{P}(t)$ is zero. Examining the equations (11)-(19), one can find that $P_i' \geq 0$ if $P_i = 0$ for each $1 \leq i \leq 9$. This implies that the non-negative octant is invariant. This proves the part 1.

If $\mathbf{P} \in H$ is an equilibrium point, then from (19), $i_2 = 0$, hence there is no interior equilibrium point. Since $i_2 = 0$, then from (18), $i_{12} = 0$; from (15), $e_2 = 0$. From (11), either $i_1 = 0$ or $s = 0$. In either case, $e_1 = 0$ from (12), which implies that $e_2 = 0$ from (13) and $i_1 = 0$ from (14). Therefore $e_1 = e_2 = i_1 = i_2 = i_{12} = 0$ holds for any equilibrium point $\mathbf{P} \in H$. From part 1, remaining components (s, r_1, r_2, x) of $\mathbf{P}$ satisfies $s + r_1 + r_2 + x = 1$. On the other hand, it is easy to check that for any (s, r_1, r_2, x) satisfying $s+r_1+r_2+x = 1$ and $s, r_1, r_2, x \geq 0$, $(s, 0, 0, 0, 0, 0, r_1, r_2, x)$ is an equilibrium point of (11)-(19).

For part 3, we observe that if $s(0) > 0$ and $i_1(0) + i_2(0) + i_{12}(0) > 0$, then $s(t)$ is strictly decreasing, $r_2(t)$ and $x(t)$ are non-decreasing. Hence the limits

$$s^{\pm} = \lim_{t\to\pm\infty} s(t), \;\; r_2^{\pm} = \lim_{t\to\pm\infty} r_2(t), \;\; x^{\pm} = \lim_{t\to\pm\infty} x(t),$$

all exist. In particular, $i_2(t) \to 0$ and $i_{12}(t) \to 0$ as $t \to \infty$ from the convergence of $r_2(t)$ at ∞. That in turn implies that when $t \to \infty$, $e_2(t) \to 0$ from (15), then $e_1(t) \to 0$ from (13). Next the convergence of e_1 and i_2 to zero yields that $i_1(t) \to 0$ as $t \to \infty$ from (14). Finally the invariance that $\sum P_i(t) = 1$ implies that $r_1(t) \to r_1^+ \equiv 1 - s^+ - r_2^+ - x^+$ as $t \to \infty$. For $t \to -\infty$, notice that $s^- > 0$, hence (11) and $s'(t) \to 0$ implies that $i_1(t) \to 0$, $i_2(t) \to 0$ and $i_{12}(t) \to 0$ as $t \to -\infty$, then $e_1(t) \to 0$ and $e_2(t) \to 0$ from (14) and (15). Again the convergence of $s(t)$, $r_2(t)$ and $x(t)$ yields the convergence of $r_1(t)$ as $t \to -\infty$. □

We remark that if some b_i or c_i is zero, then the corresponding component $e_i(t)$ or $i_{i(j)}(t)$ can have a positive limit, for example, the solution of the equation (26) in which $c_1 = 0$. Several subsystems of (11)-(19) are invariant with respect to the dynamics, and they describe different biological sub-dynamics. Here we summarize the behavior of each sub-dynamics.

3.2 LPAI-only dynamics

If $\mu = 0$, $s(0) > 0$, $e_1(0) \geq 0$, $i_1(0) > 0$, $r_1(0) \geq 0$, $e_2(0) = 0$, $i_2(0) = 0$, $i_{12}(0) = 0$, $r_2(0) = 0$, $x(0) = 0$, then $e_2(t) \equiv 0$, $i_2(t) \equiv 0$, $i_{12}(t) \equiv 0$, $r_2(t) \equiv 0$, $x(t) \equiv 0$ from the uniqueness of the solution. Hence (11)-(19) is reduced to a SEIR model with no birth/death for LPAI epidemics:

$$\begin{cases} s' = & -a_1 i_1 s, \\ e_1' = & a_1 i_1 s - b_1 e_1, \\ i_1' = & b_1 e_1 - c_1 i_1, \\ r_1' = & c_1 i_1. \end{cases} \tag{22}$$

In (22), $s(t)+e_1(t)+i_1(t)+r_1(t) = 1$, hence we only need to consider the first three equations. The dynamics of (22) is well-known, which we summarize here:

1. When $t \to \infty$, $(s(t), e_1(t), i_1(t)) \to (s_1^+, 0, 0)$;

2. The function $V_1(s, e_1, i_1) = s + e_1 + i_1 - (c_1/a_1) \ln s$ remains constant on a solution curve $(s(t), e_1(t), i_1(t))$, hence the final susceptible size s_1^+ can be determined by

$$s^0 + e_1^0 + i_1^0 - \frac{c_1}{a_1} \ln s^0 = s_1^+ - \frac{c_1}{a_1} \ln s_1^+, \tag{23}$$

   where $s^0 = s(0)$ and similar notations for other variables.

3. The basic reproduction number $\Re_{0,1} = a_1 s^0 / c_1$. If $\Re_{0,1} < 1$, then $(e_1(t)+i_1(t))' < 0$ for $t > 0$ and the infection dies out; if $\Re_{0,1} > 1$, then for some $t_0 > 0$, $(e_1(t)+i_1(t))' > 0$ for $t \in (0, t_0)$ and $(e_1(t)+i_1(t))' < 0$ for $t > t_0$, thus an outbreak occurs.

3.3 HPAI-only dynamics

If $\mu = 0$, $s(0) > 0$, $e_1(0) = 0$, $i_1(0) = 0$, $r_1(0) = 0$, $e_2(0) \geq 0$, $i_2(0) > 0$, $i_{12}(0) = 0$, $r_2(0) \geq 0$, $x(0) \geq 0$, then $e_1(t) \equiv 0$, $i_1(t) \equiv 0$, $i_{12}(t) \equiv 0$, $r_1(t) \equiv 0$ from the uniqueness of the solution. Hence (11)-(19) is reduced to a SEIR

model with no birth/death for HPAI epidemics:

$$\begin{cases} s' = & -a_2 i_2 s, \\ e_2' = & a_2 i_2 s - b_2 e_2, \\ i_2' = & b_2 e_2 - c_2 i_2, \\ r_2' = & c_2 i_2, \\ x' = & (1-p) c_2 i_2. \end{cases} \tag{24}$$

Again only the first three equations are essential, hence (24) has the same dynamical properties as (22):

1. When $t \to \infty$, $(s(t), e_2(t), i_2(t)) \to (s_2^+, 0, 0)$;
2. The function $V_2(s, e_2, i_2) = s + e_2 + i_2 - (c_2/a_2) \ln s$ remains constant on a solution curve $(s(t), e_2(t), i_2(t))$, hence the final susceptible size s_2^+ can be determined by
$$s^0 + e_2^0 + i_2^0 - \frac{c_2}{a_2} \ln s^0 = s_2^+ - \frac{c_2}{a_2} \ln s_2^+.$$
3. The basic reproduction number $\Re_{0,2} = a_2 s^0 / c_2$. If $\Re_{0,2} < 1$, then $(e_2 + i_2(t))' < 0$ for $t > 0$ and the infection dies out; if $\Re_{0,2} > 1$, then for some $t_0 > 0$, $(e_2(t) + i_2(t))' > 0$ for $t \in (0, t_0)$ and $(e_2(t) + i_2(t))' < 0$ for $t > t_0$, thus an outbreak occurs.

3.4 superinfection only dynamics

If $s(0) > 0$, $e_1(0) = e_2(0) = 0$, $i_1(0) = i_2(0) = 0$, $r_1(0) = 0$, $i_{12}(0) > 0$, $r_2(0) \geq 0$, $x(0) \geq 0$, then $e_1(t) = e_2(t) \equiv 0$, $i_1(t) = i_2(t) \equiv 0$, $r_1(t) \equiv 0$ from the uniqueness of the solution. Hence (11)-(19) is reduced to a SIR model with no birth/death:

$$\begin{cases} s' = & -a_3 i_{12} s, \\ i_{12}' = & a_3 i_{12} s - c_3 i_{12}, \\ r_2' = & c_3 i_{12}. \end{cases} \tag{25}$$

The dynamics of (25) is the one of classical Kermack-McKendrick SIR model:

1. When $t \to \infty$, $(s(t), i_{12}(t)) \to (s_3^+, 0)$;
2. The function $V_3(s, i_{12}) = s + i_{12} - (c_3/a_3) \ln s$ remains constant on a solution curve $(s(t), i_{12}(t))$, hence the final susceptible size s_3^+ can be determined by
$$s^0 + i_{12}^0 - \frac{c_3}{a_3} \ln s^0 = s_3^+ - \frac{c_3}{a_3} \ln s_3^+.$$
3. The basic reproduction number $\Re_{0,3} = a_3 s^0 / c_3$. If $\Re_{0,3} < 1$, then $i_{12}'(t) < 0$ for $t > 0$ and the infection dies out; if $\Re_{0,3} > 1$, then for some $t_0 > 0$, $i_{12}'(t) > 0$ for $t \in (0, t_0)$ and $i_{12}'(t) < 0$ for $t > t_0$, thus an outbreak occurs.

3.5 A special L-H-LH dynamics

In [29], one set of experiments is to treat animals infected by LPAI viruses as susceptible class, and animals infected by HPAI viruses as infectious class. After they conducted transmission experiments from animals infected by HPAI viruses to animals infected by LPAI viruses, they only considered the recovery from co-infected animals and HPAI virus infected animals. This setting corresponds to another subsystem of the full system (11)-(19). Suppose that $\mu = 0$ and $c_1 = 0$, and $s(0) = 0$, $e_1(0) = 0$, $e_2(0) = 0$, $r_1(0) = 0$, then these four variables remain zero for all $t \geq 0$. The system (11)-(19) is reduced to the following system:

$$\begin{cases} i_1' &= -\tau i_1 i_2, \\ i_2' &= -c_2 i_2, \\ i_{12}' &= \tau i_1 i_2 - c_3 i_{12}, \\ r_2' &= p c_2 i_2 + c_3 i_{12}, \\ x' &= (1-p) c_2 i_2. \end{cases} \tag{26}$$

The system is determined by the first 3 equations. Indeed (26) is solvable with initial value $(i_1^0, i_2^0, i_{12}^0, r_2^0, x^0)$, and the solution of the initial value problem is given by

$$\begin{aligned} i_1(t) =& i_1^0 \exp(\tau c_2^{-1} i_2^0 (\exp(-c_2 t) - 1)), \quad i_2(t) = i_2^0 \exp(-c_2 t), \\ i_{12}(t) =& \exp(-c_3 t)\Big(i_{12}^0 + \tau i_1^0 i_2^0 \int_0^t \exp[\tau c_2^{-1} i_2^0 (\exp(-c_2 s) - 1) + (c_3 - c_2)s] ds\Big), \end{aligned} \tag{27}$$

and $r_2(t)$, $x(t)$ can be integrated from (26) and form of $(i_1(t), i_2(t), i_{12}(t))$ in (27). Notice that since $c_1 = 0$, then the limit of $i_1(t)$ as $t \to \infty$ is not zero, but

$$i_1^+ = \lim_{t\to\infty} i_1(t) = i_1^0 \exp(-\tau c_2^{-1} i_2^0). \tag{28}$$

This is because (26) is essentially an SIR type model with i_1 and i_2 playing the role of susceptible class, and i_{12} being the infective class. Compared with earlier subsystems, we have

1. When $t \to \infty$, $(i_1(t), i_2(t), i_{12}(t), r_2(t), x(t)) \to (i_1^+, 0, 0, r_2^+, x^+)$.

2. There is no conserved quantity as previous subsystems, but the equation is solvable and the final size of $i_1(t)$ is given by (28). On the other hand, from the expression of $i_2(t)$, the equation of $x(t)$ and (28), we obtain

   $$x^+ = x^0 + (1-p) i_2^0, \quad \text{and } r_2^+ = i_1^0 + p i_2^0 + i_{12}^0 + r_2^0 - i_1^0 \exp(-\tau c_2^{-1} i_2^0). \tag{29}$$

   Hence the final size is completely determined.

3. The basic reproduction number is given by $\Re_{0,4} = \dfrac{\tau i_1^0 i_2^0}{c_3 i_{12}^0}$. If $\Re_{0,4} < 1$, then $i'_{12}(t) < 0$ for $t > 0$. So the co-infection dies out. If $\Re_{0,4} > 1$, there will be a outbreak of co-infection.

3.6 A complete L-H-LH dynamics

Finally we consider a subsystem without class s and e_i. Assume that $\mu = 0$, $s(0) = 0$, $e_1(0) = 0$ and $e_2(0) = 0$. Hence the system (11)-(19) becomes

$$\begin{cases} i_1' = & -\tau i_1 i_2 - c_1 i_1, \\ i_2' = & -c_2 i_2, \\ i_{12}' = & \tau i_1 i_2 + \rho i_2 r_1 - c_3 i_{12}, \\ r_1' = & c_1 i_1 - \rho i_2 r_1, \\ r_2' = & p c_2 i_2 + c_3 i_{12}, \\ x' = & (1-p) c_2 i_2. \end{cases} \tag{30}$$

Similar to (26), (30) is explicitly solvable:

$$i_1(t) = i_1^0 \exp(\tau c_2^{-1} i_2^0 (\exp(-c_2 t) - 1) - c_1 t), \quad i_2(t) = i_2^0 \exp(-c_2 t), \tag{31}$$

and other components can be also expressed but we omit the cumbersome form for the simplicity. For our purpose, we only point out that when $t \to \infty$, $(i_1(t), i_2(t), i_{12}(t), r_1(t), r_2(t), x(t)) \to (0, 0, 0, r_1^+, r_2^+, x^+)$. From (31) and the integration of the equation of $r_2(t)$, we obtain the final sizes:

$$\begin{aligned} r_1^+ =& r_1^0 \exp(-\rho c_2^{-1} i_2^0) + c_1 i_1^0 \int_0^\infty \exp[(\tau - \rho) c_2^{-1} i_2^0 \exp(-c_2 t) - \tau c_2^{-1} i_2^0 - c_1 t] dt, \\ x^+ =& x^0 + (1-p) i_2^0, \quad \text{and } r_2^+ = i_1^0 + p i_2^0 + i_{12}^0 + r_1^0 + r_2^0 - r_1^+. \end{aligned} \tag{32}$$

One can compare the final size formula in (32) with the ones in (28) and (29). In fact this comparison can be described as follows:

Proposition 3.1. *Consider the full system* (11)-(19) *with* $\mu = 0$, *and suppose the initial distribution is* $\mathbf{P}_0 = (0, 0, 0, i_1^0, i_2^0, i_{12}^0, 0, r_2^0, x^0)$, *hence the dynamics is effectively described by* (30). *Let* $(\bar{i}_1(t), \bar{i}_2(t), \bar{i}_{12}(t), \bar{r}_1(t), \bar{r}_2(t), \bar{x}(t))$ *and* $(\widetilde{i}_1(t), \widetilde{i}_2(t), \widetilde{i}_{12}(t), \widetilde{r}_1(t), \widetilde{r}_2(t), \widetilde{x}(t))$ *be the solutions to the system* (30) *with* $c_1 = 0$ *and* $c_1 > 0$ *respectively, satisfying the same initial condition* $\mathbf{P}_0$. *Let the final size of the two solutions be* $(0, 0, 0, \bar{i}_1, 0, 0, \bar{r}_2, \bar{x})$ *and* $(0, 0, 0, 0, 0, 0, \widetilde{r}_1, \widetilde{r}_2, \widetilde{x})$ *respectively. Then*

$$\bar{i}_1 + \bar{r}_2 = \widetilde{r}_1 + \widetilde{r}_2.$$

The proof is clear from calculation above since $\bar{x} = \widetilde{x}$.

3.7 Final size of the full system

To consider the final susceptible size we construct an "anti-Lyapunov function":

Proposition 3.2. *Let* $\mathbf{P}(t)$ *be a solution of* (11)-(19). *Define a function*

$$V(t) = s(t) + e_1(t) + e_2(t) + i_1(t) + i_2(t) + i_{12}(t) - K \ln s(t), \tag{33}$$

where $K = \max\{c_1/a_1, c_2/a_2, c_3/a_3\}$. *Then* $V'(t) \geq 0$.

Proof. From straight forward calculation, we obtain

$$\begin{aligned} V'(t) &= s'(t) + e_1'(t) + e_2'(t) + i_1'(t) + i_2'(t) + i_{12}'(t) - Ks'(t)/s(t) \\ &= a_1 i_1(t) \left(K - \frac{c_1}{a_1}\right) + a_2 i_2(t) \left(K - \frac{c_2}{a_1}\right) + a_3 i_{12}(t) \left(K - \frac{c_3}{a_3}\right) + \rho i_2(t) r_1(t). \end{aligned}$$

Then $V'(t) \geq 0$ from the definition of K. □

The information in Proposition 3.2 is useful in comparing the final susceptible size s^+ for the full system (11)-(19) with the ones in subsystems considered above. For example, we assume that $K = c_1/a_1$, so that LPAI has smaller basic reproduction number than HPAI and the mixed type. We assume that $s(0) > 0$, $e_1(0) \geq 0$, $i_1(0) > 0$, $r_1(0) \geq 0$, $e_2(0) = 0$, $i_2(0) = 0$, $i_{12}(0) = 0$, $r_2(0) = 0$, and $x(0) = 0$. Then in the case of $\mu = 0$, then the LPAI-only dynamics above implies that final size is given by s_1^+ in (23). On the other hand, if $\mu > 0$, then HPAI is possible, and from Proposition 3.2, we obtain

$$s^0 + e_1^0 + i_1^0 - \frac{c_1}{a_1} \ln s^0 < s^+ - \frac{c_1}{a_1} \ln s^+. \tag{34}$$

Hence in light of (23), we find that

$$s_1^+ - \frac{c_1}{a_1} \ln s_1^+ < s^+ - \frac{c_1}{a_1} \ln s^+. \tag{35}$$

This implies $s^+ < s_1^+$.

3.8 Basic reproduction number of the full system

The disease free equilibria (DFEs) are $(s^0, 0, 0, 0, 0, 0, r_1^0, r_2^0, x^0)$, where $s^0 + r_1^0 + r_2^0 + x^0 = 1$. The basic reproduction number, $\Re_0$, is an essential summary parameter. It is defined as the average number of secondary infections caused when a single infected individual is introduced into a host population where everyone is susceptible. It is know that, if $\Re_0 < 1$, then the disease free equilibrium is locally asymptotically stable; whereas if $\Re_0 > 1$, then it is unstable, and a local disease outbreak is possible. A precise mathematical definition of $\Re_0$ for one infection is the spectral radius of the next generation matrix (Diekmann and Heesterbeek [10], van den Driessche and Watmough

[30, 31]). To compute the next generation matrix for the full model (11)-(19), we only need to consider the infected compartments as follows.

$$\frac{d}{dt}\begin{pmatrix} e_1 \\ e_2 \\ i_1 \\ i_2 \\ i_{12} \end{pmatrix} = f - v = \begin{pmatrix} a_1 i_1 s \\ a_2 i_2 s \\ 0 \\ 0 \\ \tau i_1 i_2 + a_3 i_{12} s + \rho i_2 r_1 \end{pmatrix} - \begin{pmatrix} b_1 e_1 + \mu e_1 \\ b_2 e_2 - \mu e_1 \\ \tau i_1 i_2 + c_1 i_1 - b_1 e_1 \\ c_2 i_2 - b_2 e_2 \\ c_3 i_{12} \end{pmatrix},$$

where f denotes the rate of new infections and v denotes the rate of transfer (by other means) between compartments. Let F and V be the corresponding Jacobian matrices at the DFE, which linearize the system at the equilibrium point. Then $F = \begin{pmatrix} 0 & 0 & a_1 s^0 & 0 & 0 \\ 0 & 0 & 0 & a_2 s^0 & 0 \\ 0 & 0 & 0 & 0 & 0 \\ 0 & 0 & 0 & 0 & 0 \\ 0 & 0 & 0 & \rho r_1^0 & a_3 s^0 \end{pmatrix}$, and $V = \begin{pmatrix} b_1+\mu & 0 & 0 & 0 & 0 \\ -\mu & b_2 & 0 & 0 & 0 \\ -b_1 & 0 & c_1 & 0 & 0 \\ 0 & -b_2 & 0 & c_2 & 0 \\ 0 & 0 & 0 & 0 & c_3 \end{pmatrix}$. Then,

$$V^{-1} = \begin{pmatrix} \frac{1}{b_1+\mu} & 0 & 0 & 0 & 0 \\ \frac{\mu}{(b_1+\mu)b_2} & \frac{1}{b_2} & 0 & 0 & 0 \\ \frac{b_1}{(b_1+\mu)c_1} & 0 & \frac{1}{c_1} & 0 & 0 \\ \frac{\mu}{(b_1+\mu)c_2} & \frac{1}{c_2} & 0 & \frac{1}{c_2} & 0 \\ 0 & 0 & 0 & 0 & \frac{1}{c_3} \end{pmatrix},$$

and the next generation matrix is given by

$$FV^{-1} = \begin{pmatrix} \frac{a_1 b_1 s^0}{(b_1+\mu)c_1} & 0 & \frac{a_1 s^0}{c_1} & 0 & 0 \\ \frac{a_2 \mu s^0}{(b_1+\mu)c_2} & \frac{a_2 s^0}{c_2} & 0 & \frac{a_2 s^0}{c_2} & 0 \\ 0 & 0 & 0 & 0 & 0 \\ 0 & 0 & 0 & 0 & 0 \\ \frac{\rho r_1^0 \mu}{(b_1+\mu)c_2} & \frac{\rho r_1^0}{c_2} & 0 & \frac{\rho r_1^0}{c_2} & \frac{a_3 s^0}{c_3} \end{pmatrix}.$$

Hence the basic reproduction number of the full system (11)-(19) is given by the spectral radius of the matrix FV^{-1}, which is

$$\max\left\{\frac{a_1 b_1 s^0}{(b_1+\mu)c_1}, \frac{a_2 s^0}{c_2}, \frac{a_3 s^0}{c_3}\right\}. \tag{36}$$

We interpret the matrices above and the basic reproduction number in a biological meaningful way. The diagonal entries of the matrix V^{-1} have the

interpretation of the average waiting time. Once an individual animal enters into the latent stage E_l, it will spend the average length of time $\frac{1}{b_1+\mu}$ in this stage, transit to the stage E_h with probability $\frac{\mu}{b_1+\mu}$, and transit to the stage I_l with probability $\frac{b_1}{b_1+\mu}$, and transit to the I_h with probability $\frac{\mu}{b_1+\mu}$. Similarly if an individual enters into the latent stage E_h, it will spend the average length of time $\frac{1}{b_2}$ and $\frac{1}{c_2}$ in the stages E_h and I_h respectively. Also if an individual enters into the infectious stage I_l (or I_h, or I_{lh}), it will spend the average length of time $\frac{1}{c_1}$ (or $\frac{1}{c_2}$, or $\frac{1}{c_3}$) in this infectious stage.

The entries of the matrix F have the interpretation of the reproduction rate. For example, $a_1 s^0$ is the rate at which I_l infected individuals produce new infections into the compartment E_l; $a_2 s^0$ is the rate at which I_h infected individuals produce new infections into the compartment E_h. Most interestingly, I_h infected individuals produce new infections into the compartment I_{lh}, co-infections, at the rate ρr_1^0.

The (i, j) entry of the matrix FV^{-1} is the expected number of new infections in the compartment i produced by the infected individual original entered into compartment j. When one infected individual is introduced into the compartment E_l, the number $\frac{a_1 b_1 s^0}{(b_1+\mu)c_1}$ is the average number of secondary infections in the compartment E_l that occur; the number $\frac{a_2 \mu s^0}{(b_1+\mu)c_2}$ is the average number of secondary infections in the compartment E_h that occur; the number $\frac{\rho r_1^0 \mu}{(b_1+\mu)c_2}$ is the average number of secondary infections in the compartment E_{lh} that occur. When one infected individual is introduced into the compartment E_h, the average number of secondary infections occur in this compartment is $\frac{a_2 s^0}{c_2}$. When one infected individual is introduced into the compartment I_{lh}, the average number of secondary infections occur in this compartment is $\frac{a_3 s^0}{c_3}$.

If we consider three different infections together in our full system, then the basic reproduction rate will be the spectral radius of the matrix FV^{-1}, which is given in (36). From the biological significance of the entries of the matrix FV^{-1}, if $\mu = 0$, and view these three infections separately, each infection (LPAI, HPAI and mixed) has it own basic reproduction rate, described in subsections 3.2-3.4:

$$\Re_{0,1} = \frac{a_1 s^0}{c_1}, \quad \Re_{0,2} = \frac{a_2 s^0}{c_2}, \quad \Re_{0,3} = \frac{a_3 s^0}{c_3}.$$

However, the next generation matrix gives us more information about subthreshold for each infection within the whole dynamics of the full model. From the biological interpretation, we can see that the entries in the first column of the matrix FV^{-1} sever as the thresholds of infection spreading. For example, for the low pathogenicity avian influenza virus, $\overline{\Re}_l = \frac{a_1 b_1 s^0}{(b_1+\mu)c_1}$; for the high pathogenicity avian influenza virus, $\overline{\Re}_h = \frac{a_2 \mu s^0}{(b_1+\mu)c_2}$; and for the co-infection, $\overline{\Re}_{lh} = \frac{\rho r_1^0 \mu}{(b_1+\mu)c_2}$. If $\mu = 0$, then $\overline{\Re}_h = 0$. This is biologically significant. It indicates the emergency of high pathogenicity infection from

spreading of low pathogenicity avian influenza. To establish the co-infection, the outbreak of low pathogenicity avian influenza is necessary, since it requires $\mu \neq 0$ and $r_1^0 \neq 0$.

For the application of basic reproduction number defined in [30, 31], we cautiously point out that the disease-free equilibrium in [30, 31] is unique and asymptotically stable for the disease-free system. This is not satisfied in our system, but nevertheless the setting in [30, 31] can be applied in this particular model with same biological meaning.

Parameter names	Parameters	Values	Units
LPAI virus infection rate	a_1	1	1/day
LPAI virus latent period	$1/b_1$	2	day
LPAI virus infectious period	$1/c_1$	4.8	day
HPAI virus infection rate	a_2	15	1/day
HPAI virus latent period	$1/b_2$	4	day
HPAI virus infectious period	$1/c_2$	3.5	day
Co-infection rate	a_3	1.7	1/day
Co-infectious period	$1/c_3$	3.5	day
Death rate	p	0.02	none
HPAI infecting LPAI rate	τ	0.7	1/day
HPAI infecting LPAI recovered rate	ρ	1	1/day
LPAI virus mutating to HPAI viruses	μ	1/100 - 1/1000	1/day

Table 1: Table of parameters used in numerical simulation.

4 Comparison of the model predictions and experimental data

In [29] the first set of experiments were conducted by J. A. Van Der Goot, et al. were four replicate experiments with LPAI H5N2 isolated from an outbreak in Pennsylvania in 1983. They housed chickens in cages. In each cage five chickens were inoculated at day 0. After 24 hours, they added five susceptible contact chickens. During the first 7 days they tested infection every day; and after day 7, they tested it twice a week. In [29] they used statistical tools such as generalized linear model to analyze the data. They obtained values of the transmission parameter and infectious period, and they estimated the length of the latent period. Here we choose the parameter values within the ranges of the parameter values in [29], see Table 1.

As we show in Section 3, our full model (11)-(19) can induce a submodel on LPAI dynamics, which is given by the system (22). Fig. 2-A shows the comparison between the submodel (22) and the experimental data in [29]. The latent chickens and infectious chickens were not distinguished in their time series data. For the purpose of comparison, we plot the summation of the

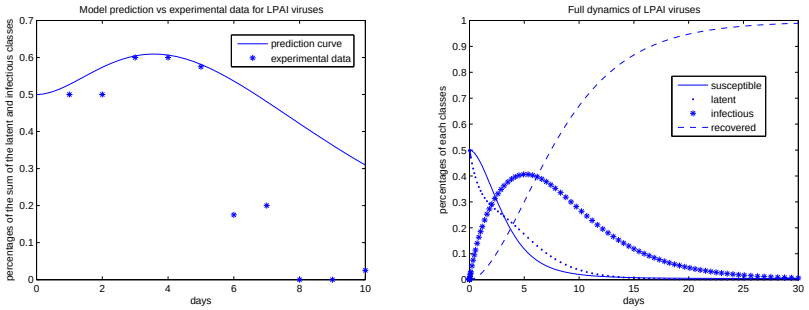

Figure 2: Comparison of the LPAI submodel model (22) and the data in [29]. (A) Left: Predictions from (22) and experimental data; (B) Right: The full dynamics of 22. The missing data is taken to be zero. Initial conditions are half latent and half susceptible as in the experiments.

latent chickens and infectious chickens. Keeping the same initial conditions as they are in experiments, we plot the full dynamics of the submodel on LPAI (22) in Figure 2-B.

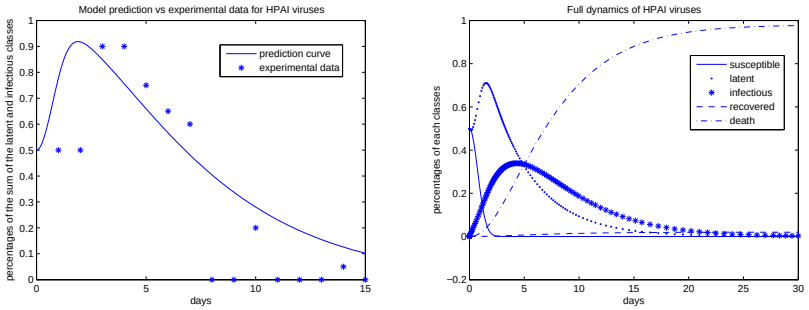

Figure 3: Comparison of the HPAI submodel model (24) and the data in [29]. (A) Left: Predictions from (24) and experimental data; (B) Right: The full dynamics of 24. The missing data is taken to be zero. Initial conditions are half latent and half susceptible as in the experiments.

The second set of experiments were two replicate experiments with the corresponding HPAI H5N2. Our full model also can induce a submodel on the dynamics of the HPAI, which is given by the system (24). We choose the parameter values from the ranges of the corresponding parameter given in [29]. The comparison between the experimental data and the submodel predictions are showed in Fig. 3-A. Keeping the same initial conditions as they are in experiments, we plot the full dynamics of the submodel on HPAI 24 in Figure 3-B.

Comparing Figure 2-B and Figure 3-B, we can see the following

differences. For LPAI the number of the latent animals drop down from the beginning. But, for HPAI the number of the latent animals increase, and after it reaches a maximum the number drop down. This gives HPAI more chances to spread. Although the infected patterns are similar, most of animals infected by LPAI are recovered while most of animals infected by HPAI are dead. So, animals infected by HPAI are more infectious then animals infected by LPAI. This is the answer to the second question in the Introduction.

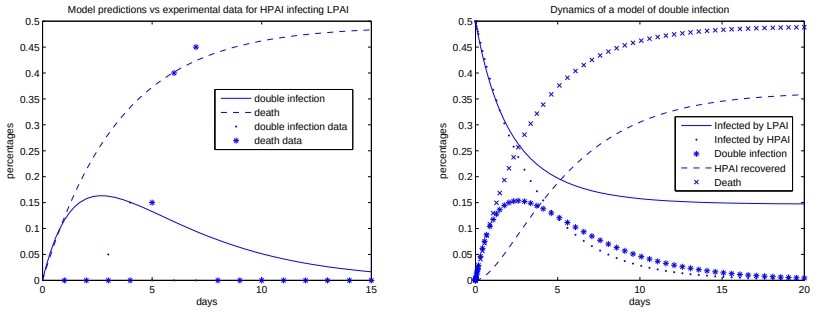

Figure 4: Comparison of the HPAI submodel model (26) and the data in [29]. (A) Left: Predictions from (24) and experimental data; (B) Right: The full dynamics of 26. The missing data is taken to be zero. Initial condition are half LPAI chickens and half HPAI chickens as in the experiments.

The third set of their experiments are two replicate experiments with the HPAI H5N2 taking contact chickens to be already infected by LPAI. There were a large amount of chickens that had died during the experiments. We take this fact into account. Since in the experiments they did not count the recovered animals from LPAI, we also don't count them in this submodel, which is given by the system (26). This submodel is also induced for our full model. Fig. 4-A shows a comparison between the experimental results and the model results.

If we also take the recovery of the animals infected by LPAI into account, we need to use the submodel (30), which is also induced from the full model. Some details of the dynamics will be different from that of the submodel (26). All chickens infected by LPAI will be recovered eventually, and some of them move to the LPAI recovered compartment, and some move to the HPAI recovered compartment. As Proposition 3.1 states, the summation of the infected by LPAI treated as the susceptible class and the HPAI recovered and the summation of the LPAI recovered class and HPAI recovered class are the same, although two quantities of HPAI recovered classes are different. To compare the differences between these two submodels, we plot each component for each submodel. Fig. 4-B shows the dynamics of the submodel 26, and Fig. 5-A shows dynamics of the submodel of (30). Whichever model for the superinfection is chosen, the basic feature of the superinfection

is similar. Although the number of the double infected animals increase first and then decrease, the maximum value is much lower than that where susceptible animals are not infected by LPAI. So animals previously infected by LPAI are protected against infection with HPAI. We answered the third question in the Introduction.

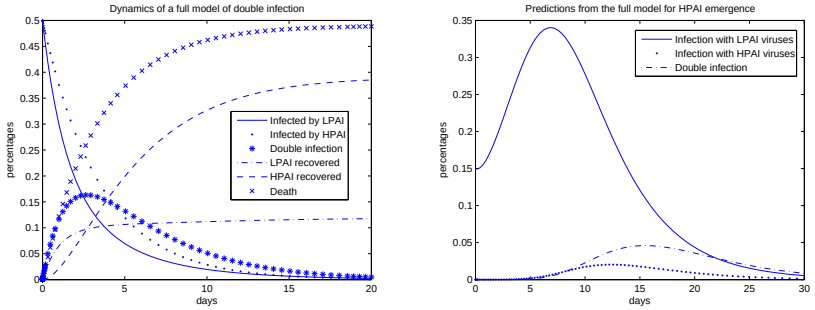

Figure 5: (A) Left: The full dynamics of the submodel (30); (B) Right: Emergence of HPAI viruses from an outbreak of LPAI viruses. The initial conditions are $s(0) = 0.8$, $e_1(0) = 0.05$, $i_1(0) = 0.15$, and the rest are all zeroes.

In order to answer the rest three questions, we need computational results from our full model. The experiments done by [29] give no information about the mutation of LPAI viruses. From some literature [4, 14], we know it takes 3 months or half year to evolve HPAI viruses for LPAI viruses outbreak. Therefor we take a value of the mutation parameter μ to be about $1/100 - 1/1000$ over a day. From our computational study, when the infection with LPAI viruses is currently circulating in a population, the infection with HPAI viruses could spread in a very low level. This spreading actually depends on the initial state of the infection with LPAI viruses in the population. Figure 5-B shows one result with a specific initial conditions. This figure also shows how HPAI viruses emerge from an outbreak of LPAI viruses. It also shows that superinfection occurs.

To answer the last question, we choose different initial conditions for the portion of the infection with LPAI viruses. One computation result shows that the level of HPAI viruses infection will go as low as $1/1000$ if the initial condition for the portion of the infection with LPAI viruses is $40/100$.

5 Conclusions

We build a mathematical model to study the complexity phenomenon that high pathogenicity avian influenza virus emerges from outbreaks with low pathogenicity avian influenza virus. It may be more interesting to use stochastic models to study the experimental results in [29] since the population size was small. However, we want to consider more general

situations. We then still keep in continuous model framework. The model is based on traditional epidemiology model. The model has several submodels which can be used to explain each set of experiments in [29]. Its purpose is to explain how high pathogenicity avian influenza virus emerge from outbreaks of low pathogenicity avian influenza virus. We integrate all transmission characters of low and high pathogenicity avian influenza viruses into the model. We thus could answer basically important questions about avian influenza virus evolution. However, we did not consider long-term population dynamics. Since the experiments with H5N2 only last two weeks or one month, and even in natural setting an outbreak last one month to three month, it is reasonable to study a short-term model without birth firstly. Secondly, we only use experimental data to estimate parameter values when we conduct computational study. It is important to use natural data when we apply the model to predict real pandemics.

Mathematically the system we propose here (11)-(19) is an epidemic model with multiple parallel infectious groups, see some similar models in [9, 22]. It is shown in Section 3 that (11)-(19) possesses two SEIR subdynamics and one SIR subdynamics through parallel infectious channels. But on the other hand, the superinfection between different channels make our model more complicated than the canonical ones in [9, 22]. We noticed a PDE version of the model was numerically studied [26].

6 Acknowledgements

J.P. Tian would like to acknowledge the supports DMS-1446139 of NSF of US and NNSF of China 11371048. J Cui would like to acknowledge the support of NNSF of China 11371048.

References

[1] D.J. Alexander, A review of avian influenza in different bird species. *Vet. Microbiol.* **74** (2000) 3–13.

[2] D.J. Alexander, An overview of the epidemiology of avian influenza. *Vaccine* **25** (2007) 5637–5644.

[3] R. M. Anderson, R. M. May, Infectious Diseases of Humans: Dynamics and Control. Oxford University Press, Oxford, 1991.

[4] W. J. Bean, Y. Kawaoka, J. M. Wood, J. E. Pearson, and R. G. Webster, Characterization of virulent and avirulent A/Chicken/Pennsylvania/83 influenza A viruses: potential role of defective interfering RNAs in nature. *J. Virol.* **54** (1985) 151-160.

[5] J. Belser, K. Gustin, M. Pearce, T. Maines, H. Zeng, C. Pappas, X. Sun, P. Carney, J. Villanueva, J. Stevens, J. Katz and T. Tumpey, Pathogenesis and transmission of avian influenza A (H7N9) virus in ferrets and mice, *nature* **501** (2013), 556–559.

[6] L. Bourouibaa, A. Teslyab, and J. Wu, Highly pathogenic avian influenza outbreak mitigated by seasonal low pathogenic strains: Insights from dynamic modeling, *J of Theor Biol*, **271**, (2011) 181201.

[7] F. Brauer, Compartmental models in epidemiology. In "Mathematical epidemiology", 19–79, *Lecture Notes in Math.*, **1945**, Springer, Berlin, 2008.

[8] I. Capua, F. Mutinellia, M. D. Pozzab, I. Donatellic, S. Puzellic, F. M. Cancellottid, The 1999-2000 avian influenza (H7N1) epidemic in Italy: veterinary and human health implications. *Acta Tropica*, **83** (2002) 7-11.

[9] P. De Leenheer, S. S. Pilyugin, Multi-strain virus dynamics with mutations: A global analysis. *Math. Med. and Biol* **25**, (2008), 285–322.

[10] O. Diekmann, J.A.P. Heesterbeek, Mathematical Epidemiology of Infectious Diseases: Model Building, Analysis and Interpretation. Wiley, New York, 1999.

[11] N. M. Ferguson, A. P. Galvani, R. M. Bush, Ecological and immunological determinants of influenza evolution. *Nature* **422**, (2003), 428-433.

[12] N. M. Ferguson, C. Fraser, C. A. Donnelly, A. C. Ghani, R. M. Anderson, Public Health Risk from the Avian H5N1 Influenza Epidemic. *Science* **304** (2004) 968–969.

[13] N. M. Ferguson, D. A. T. Cummings, S. Cauchemez, et. al., Strategies for containing an emerging influenza pandemic in Southeast Asia. *Nature* **437** (2005), 209-214.

[14] M. Garcia, J. M. Crawford, J. W. Latimer, et al., 1996. Heterogeneity in the haemagglutinin gene and emergence of the highly pathogenic phenotype among recent H5N2 avian influenza viruses from Mexico. *Journal of General Virology*, **77** (1996), 1493–1504.

[15] H. Guo, M. Y. Li, Z. Shuai, A graph-theoretic approach to the method of global Lyapunov functions. *Proc. Amer. Math. Soc.* **136** (2008), no. 8, 2793–2802.

[16] H.W. Hethcote, A thousand and one epidemic models. In "Frontiers in Theoretical Biology", S. A. Levin ed., *Lecture Notes in Biomath.* **100**, Springer-Verlag, Berlin, 1994, 504–515.

[17] H. W. Hethcote, The mathematics of infectious diseases. *SIAM Rev.* **42** (2000), no. 4, 599–653.

[18] V. Hnaux, M.D. Samuel, and C.M. Bunck, Model-based evaluation of highly and low pathogenic avian influenza dynamics in wild birds, *PLoS One*, 2010; 5(6): e10997.

[19] S. Iwami, Y. Takeuchi, X. Liu, Avian-human influenza epidemic model. *Math. Biosci.* **207** (2007), no. 1, 1–25.

[20] S. Iwami, Y. Takeuchi, X. Liu, Avian flu pandemic: Can we prevent it? *Jour. Theo. Biol.* **257** (2009), no. 1, 181–190.

[21] A. Korobeinikov, Lyapunov functions and global properties for SEIR and SEIS epidemic models. *Math. Med. Biol.* **21**, (2004), 75-83.

[22] A. Korobeinikov, Global properties of SIR and SEIR epidemic models with multiple parallel infectious stages. *Bull. Math. Biol.* **71** (2009), no. 1, 75–83.

[23] A. Korobeinikov, P. K. Maini, A Lyapunov function and global properties for SIR and SEIR epidemiological models with nonlinear incidence. *Math. Biosci. Eng.* **1** (2004), no. 1, 57–60.

[24] M. Y. Li, J. R. Graef, L. Wang, J. Karsai, Global dynamics of a SEIR model with varying total population size. *Math. Biosci.* **160** (1999), no. 2, 191–213.

[25] M. Y. Li, J. S. Muldowney, Global stability for the SEIR model in epidemiology. *Math. Biosci.* **125** (1995), no. 2, 155–164.

[26] S. Liao, J. Wang, J. P. Tian, On a computational study of avian influenza. Accepted by *Discrete and Continuous Dynamical Systems*, Sept. 2009.

[27] J. Lucchetti, M. Martcheva, An avian influenza model and its fit to human avian influenza cases, in "Advances in Disease Epidemiology", J.M. Tchuenche and Z. Mukandavire, Eds. Nova Science Publishers, New York, 2009, 1–30.

[28] L. Sims, C. Narrod. Understanding avian influenza – a review of the emergence, spread, control, prevention and effects of Asian-lineage H5N1 highly pathogenic viruses. Food and Agriculture Organization of the United Nations (FAO) document, (2007) http://www.fao.org/avianflu/documents/key_ai/key_book_preface.htm

[29] J.A. van der Goot, M.C.M. De Jong, G. Koch, M. Van Boven. Comparison of the transmission characteristics of low and high pathogenicity avian influenza A virus (H5N2). *Epidemiol. Infect.* **131** (2003), 1003–1013.

[30] P. van den Driessche, J. Watmough, Reproduction numbers and sub-threshold endemic equilibria for compartmental models of diseases transmission. *Math. Biosci.* **180** (2002), 29–48.

[31] P. van den Driessche, J. Watmough, Further notes on the basic reproduction number. In "Mathematical epidemiology", 159–178, *Lecture Notes in Math.*, **1945**, Springer, Berlin, 2008.

[32] R.G. Webster, W.J. Bean, O.T. Gorman, T.M. Chambers, Y. Kawaoka. Evolution and ecology of influenza A virus. *Microbiol Rev* **56** (1992), 152-179.

Received July 2015; revised October 2015.

email: journal@monotone.uwaterloo.ca
http://monotone.uwaterloo.ca/∼journal/